JGR Atmospheres

RESEARCH ARTICLE
10.1029/2022JD037873

Temperature-Precipitation Scaling Rates: A Rainfall Event-Based Perspective

Alexis Pérez Bello[1], Alain Mailhot[1], Dominique Paquin[2], and Danahé Paquin-Ricard[3]

[1]Institut National de la Recherche Scientifique, Centre Eau Terre Environnement (INRS-ETE) Québec, Quebec City, QC, Canada, [2]Consortium on Regional Climatology and Adaptation to Climate Change (Ouranos), Montréal, QC, Canada, [3]Environment and Climate Change Canada, Montréal, QC, Canada

Key Points:

- Temperature-precipitation scaling of 1-hr annual maxima and total rainfall depth of the associated Rainfall event (RE) was investigated
- Rainfall type (stratiform or convective) of the RE plays a crucial role and should be considered in the scaling estimation
- Super Clausius-Clapeyron scaling observed in the southern regions is explained by a change in the rainfall type with increasing temperature

Supporting Information:

Supporting Information may be found in the online version of this article.

Correspondence to:

A. Pérez Bello,
Alexis.Perez_Bello@inrs.ca

Citation:

Pérez Bello, A., Mailhot, A., Paquin, D., & Paquin-Ricard, D. (2022). Temperature-precipitation scaling rates: A rainfall event-based perspective. *Journal of Geophysical Research: Atmospheres*, *127*, e2022JD037873. https://doi.org/10.1029/2022JD037873

Received 19 SEP 2022
Accepted 18 NOV 2022

Abstract The intensity of extreme rainfall is expected to increase in a future climate at a rate close to 7%/°C estimated from the Clausius-Clapeyron (CC) relationship, which represents the rate of change of the atmospheric water holding capacity with temperature. Previous studies using fixed-interval extremes (e.g., hourly or daily) have shown that extreme rainfall can also respond to temperature increases at a rate larger than the CC scaling (super CC scaling). Temperature-precipitation scaling rates (TPSR) were estimated through an event-based analysis for the Northeastern North American (NNA) region, using a 50-member large ensemble of climate simulations over the 1956–2099 period. Rainfall events (REs), in which 1-hr annual maximums (AMs) are embedded, were analyzed. Results show that the TPSR of the RE peak intensity is determined by the duration of the RE in which they are embedded. Rainfall event duration, indicative of rainfall types (large-scale or convective), therefore plays an essential role and should be considered when estimating the TPSR. Super CC scaling observed for 1-hr AM in southern regions of the domain was explained by a change in the dominant rainfall type. This study also confirms previously reported results that the more extreme 1-hr AM will be part of a shorter and probably more convective dominant RE in a future climate.

Plain Language Summary In a future climate, the extreme rainfall events are expected to be around 7% more intense for each Celsius-degree temperature increment, based on a thermodynamic relationship described by the Clausius-Clapeyron (CC) equation. Although this value can be used as a guide for many applications, numerous studies have found values higher than the one defined by this relation. This work addressed the link between Rainfall event (RE) and temperature through an event-based analysis. A duration-based classification of the extreme REs simulated by 50-member climate simulations was used. The study area covers the Northeastern North American region and the study period goes from 1956 to 2099. It was shown that the peak value and the total rainfall depth of the REs respond differently to temperature. The duration of a RE is crucial and should be taken into consideration for future temperature-precipitation scaling rate analysis. Values above the CC relation were observed in the southern regions for most of the ranges of rainfall durations analyzed. It was also found that in a future climate, the more extreme 1-hr Annual Maximums will be embedded in shorter and likely more convective dominant REs, confirming previous studies.

1. Introduction

According to the Clausius–Clapeyron (CC) relationship, the water holding capacity of the atmosphere will increase at a rate of around 7%/°C under warming conditions, hereafter called the CC scaling rate (Trenberth et al., 2003). Extreme rainfall events are therefore expected to follow this rate in a future climate, assuming that: (a) they are mainly conditioned by the available precipitable water in the atmosphere; (b) the relative humidity remains almost constant, and (c) no significant change in the atmospheric circulation patterns will occur (Lenderink & Meijgaard, 2008). However, different studies (using observational datasets and models) have shown various responses of extreme rainfall to temperature changes. These responses range from monotonous increasing trends (below, around, and over the CC scaling) to decreasing trends, or even monotonous increasing trends with a plateau or followed by a decreasing trend at higher temperatures (Berg et al., 2009; Drobinski et al., 2016; Hardwick Jones et al., 2010; Lenderink & Meijgaard, 2008; Lenderink et al., 2011; Maeda et al., 2012; Mishra et al., 2012; Panthou et al., 2014; Utsumi et al., 2011; Westra et al., 2014).

Reported scaling larger than the CC rate (hereafter called super CC scaling) has been the subject of numerous papers. Lenderink and Meijgaard (2009), Lenderink and Meijgaard (2010) argued that the super CC scaling was

associated with some basic physical process of convective events (latent heat release increases with temperature increments intensifying the updrafts on convective clouds). According to another hypothesis proposed by Haerter and Berg (2009), super CC can be explained by the transition from a scaling dominated by large-scale events at lower temperatures to one dominated by convective rainfall at higher temperatures and is related to a shift from more dominant large-scale to more convective rainfalls. Therefore they proposed that the coexistence of both precipitation types can explain the super CC.

Berg and Haerter (2013) investigated the scaling of large-scale and convective rainfalls independently (obtained from synoptic weather types or synoptic codes) by using observations in Germany. They showed that super CC scaling is observed for some temperature ranges for both rainfall types and total rainfall (convective + large-scale). These authors also found that the observed super CC scaling for total rainfall results from changes in the dominant processes involved in rainfall generation as temperature increases, supporting the hypothesis of the statistical mixture of rainfall types proposed by Haerter and Berg (2009). Molnar et al. (2015), based on observations records in Switzerland, found higher scaling rates for convective events (between 8% and 9%/°C) than for stratiform ones (between 6% and 7%/°C) but smaller than those obtained when both rainfall types were considered (between 11% and 13%/°C). These results highlight the strong influence of rainfall types on scaling and how the coexistence of stratiform and convective components can explain the departure from CC scaling as proposed by Haerter and Berg (2009).

Park and Min (2017) found that the fraction of convective rainfall plays an essential role in shaping the scaling relationship over South Korea. These authors observed that the transition from CC to super CC scaling occurs when the fraction of convective events reaches a value close to 0.2 (similar to the one reported in Germany by Berg et al., 2013). Classification of precipitation into convective or stratiform categories was based on observations of dominant cloud type. These authors also found that convective rainfall was more sensitive to variations in temperature than stratiform events (twice the CC scaling for convective events compared to values close to the CC scaling for temperature above 12°C for stratiform events). Their results support the hypothesis that both, statistical effect or statistical mixture of rainfall types (Haerter & Berg, 2009) and physical process (Lenderink & Meijgaard, 2009, 2010) contribute to super CC for the studied region. Ivancic and Shaw (2016) found that the statistical effects were the main driver of the observed super CC in most cases over the northeastern U.S. In some sites, super CC was related to physical processes, and in a small number of sites, to the coexistence of both mechanisms.

The separation of rainfall types into stratiform and convective-dominated REs is therefore important to study the temperature-precipitation relationship, especially when super CC scaling is observed. Many methods have been proposed to differentiate rainfall types such as those using synoptic weather types (or synoptic codes) (Berg & Haerter, 2013), weather conditions and/or cloud observations (Berg et al., 2013; Chernokulsky et al., 2019; Park & Min, 2017; Rulfová & Kyselý, 2013; Ye et al., 2017), lightning occurrence (Gaál et al., 2014; Ivancic & Shaw, 2016; Molnar et al., 2015), event intensity and duration (Hand et al., 2004; Hatsuzuka et al., 2021; Loriaux et al., 2013; Panthou et al., 2014), radar observations (Llasat et al., 2005; Penide et al., 2013; Rigo & Llasat, 2004), rainfall observations (using the distribution of rainfall amount as a function of the rainfall rate) (Martinkova & Hanel, 2016; Ruiz-Leo et al., 2013; Tremblay, 2005), based on simulations from regional climate models (RCM) (Fischer et al., 2015; Kyselý et al., 2016), or even using manual classifications (Kunkel et al., 2012).

The Large Ensemble (50 members) of regional climate simulations from the fifth version of the Canadian Regional Climate Model (CRCM5-LE) was considered for the present study (Leduc et al., 2019; Martynov et al., 2013; Šeparović et al., 2013). Pérez Bello et al. (2021) (hereafter PB21), using the CRCM5-LE simulations, estimated the TPSRs at different time scales and intensities for historical and future climate with surface air temperature (SAT) or surface dew point temperature (SDPT) as a covariate. Fixed-interval (e.g., 1 hr or 24 hr) annual maximum (AM) values were analyzed. These authors found a super CC scaling in the southern part of the Northeastern North American (NNA) domain when SDPT was considered. However, the hydrological impact of the related REs depends on their characteristics, such as the peak value, the duration and total rainfall generated by the RE (Gaál et al., 2014). Using only the AM value to assess the potential hydrological consequences of rainfall implies that a significant part of this event is not considered. Furthermore, AM values with the same intensities could be related to different REs and hydrological responses. This paper extends the previous work carried out by PB21 and studies the Temperature-precipitation scaling rates (TPSR) from a large ensemble of RCM simulations

through an event-based analysis. It shows that event-based analysis provides a unique perspective on scaling, allowing storm types to be separated.

A duration-based classification of the extreme REs simulated by the CRCM5-LE was realized. This classification is used to separate rainfall types and addresses the three following questions:

1. Does the 1-hr maximum intensity of REs scale at the same rate as the total rainfall depth of the event in which it is embedded?
2. What is the impact of rainfall duration on the temperature-precipitation scaling rate (TPSR)?
3. Is super CC observed in REs of different durations?

2. Data Sets and Methods

2.1. CRCM5-LE

The CRCM5-LE dynamically downscaled the 50-member Canadian Earth System Model version 2 (Arora et al., 2011)—Large Ensemble (CanESM2-LE) (Fyfe et al., 2017; Sigmond et al., 2018). CanESM2-LE uses observed greenhouse, aerosols and land-use emissions up to 2005 and the radiative forcing scenario RCP8.5 (Representative Concentration Pathways) (Riahi et al., 2011; van Vuuren et al., 2011) from 2006 to 2099. This ensemble covers the NNA region with a spatial resolution of 0.11° (around 12 km) over the 1950–2099 period. The period from 1950 to 1955 was discarded as a spin-up period. The CRCM5-LE uses the deep convection parameterization from Kain and Fritsch (1990), the shallow convection based on the Kuo (Kuo, 1965) transient scheme (Bélair et al., 2005) and the large-scale precipitation is diagnosed by the Sundqvist (1978), Sundqvist et al. (1989) condensation scheme. Further details about the CRCM5-LE can be found in Leduc et al. (2019).

Three simulated variables from the CRCM5-LE were used: (a) 3-hr SAT, (b) 3-hr surface relative humidity, (c) 1-hr precipitation. Three-hour SAT series and 3-hr surface relative humidity were used to estimate the 3-hr SDPT using the equation proposed by Alduchov and Eskridge (1996), Lawrence (2005) (see PB21 Supporting Information S1). Average seasonal (May–September) SDPTs were estimated from the corresponding 3-hr series.

2.2. Rainfall Events

Rainfall events (RE) are defined by specifying a minimum dry period or minimum inter-event time (MIT) before and after each event and a threshold above which the period (e.g., hour, day) is considered as "wet." Dunkerley (2008) reported the different MIT values, ranging from 3 min to 24 hr, used in various applications and contexts. Most recent studies related to the temperature-precipitation relationship, considered for instance MIT values of 6 min (Visser et al., 2020), 1 hr (Gao et al., 2018; Wasko et al., 2018), 2 hr (Gaál et al., 2014; Molnar et al., 2015), 3 hr (Hatsuzuka et al., 2021; Visser et al., 2021; Wasko et al., 2015), 5 hr (Wasko & Sharma, 2014), and 6 hr (Panthou et al., 2014). Sensitivity analysis carried out by Panthou et al. (2014) showed no significant impact of MIT and threshold on the TPSRs results. Similar conclusions were obtained by Hatsuzuka et al. (2021), who considered different MIT values.

REs associated with 1-hr AMs rainfall over the May to September period were considered (hereafter called 1-hr AM RE). REs were selected by first identifying the 1-hr AM and then the RE in which each 1-hr AM is embedded. A 3-hr MIT (Hatsuzuka et al., 2021) along with a 0.1 mm threshold (Dunkerley, 2015; Svoboda et al., 2017) to separate "dry" and "wet" hours were used. A 3-hr MIT was selected to avoid large intra-event intermittencies and preserve the extreme RE character (e.g., storm duration) (Gaál et al., 2014). Figure 1 shows examples of REs for a given year. Two characteristics of the 1-hr AM RE were analyzed: event duration and total rainfall depth.

1-hr AM REs were classified into short- (<5 hr) (SDE), mid- (from 5 to 10 hr) (MDE) and long- (>10 hr) (LDE) duration events based on the categories proposed by Hatsuzuka et al. (2021). It is assumed that SDE can be associated with dominant convective rainfall, LDE with dominant synoptic-scale storms, and MDE combines both storm types. However, it is also possible to find convective systems embedded in LDE (Hatsuzuka et al., 2021). RE duration is used as a proxy of rainfall types.

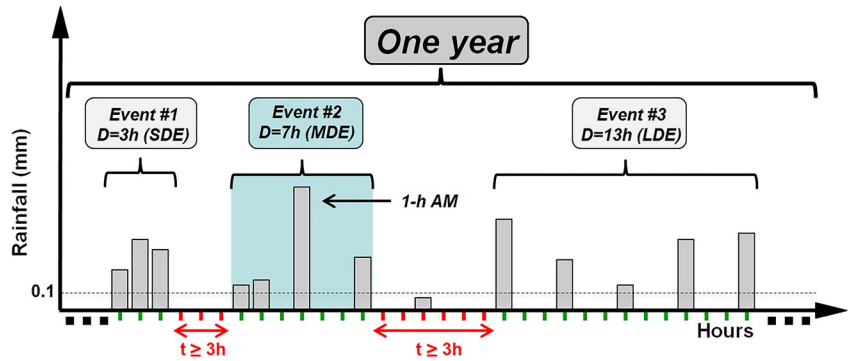

Figure 1. Diagram showing the partition of an hourly precipitation series into rainfall events for a given year. The threshold considered to define a "wet" hour is set to 0.1 mm, and the minimum dry duration between events is set to 3 hr. The 1-hr AM and the corresponding RE (event #2) are shown.

2.3. Scaling Estimation Method

Quantile regression (QR) (Koenker, 2005; Koenker & Bassett, 1978) was applied to estimate the TPSRs, as proposed by Wasko and Sharma (2014) and the R package "quantreg" (Koenker et al., 2022) was used. QR links conditional quantiles of the response variable distribution to specific predictor variables, while in standard linear regression, the conditional response of the mean value is estimated. QR was preferred since it is more flexible in representing the extreme precipitation response for different intensity levels (Li, Zwiers, Zhang, Chen, et al., 2019). The QR was applied using the following equation (Ali et al., 2018; Wasko et al., 2015):

$$\log P = \beta_0^{(q)} + \beta_1^{(q)} T \tag{1}$$

where q is the percentile (e.g., 50th or 99th), P corresponds to the 1-hr AM or total rainfall depth, T to the average seasonal (Zhang et al., 2017) (May–September) SDPT, $\beta_0^{(q)}$ and $\beta_1^{(q)}$ are the parameters of the QR. SPDT was considered in this study, as more robust estimates of TPSR can be obtained compared to when using SAT (Pérez Bello et al., 2021). The TPSR for a given percentile q was calculated differently depending if duration was considered or not. When duration was not considered (NC for No Covariate), the TPSR for AMs and total rainfall depth used the exponential transformation of the regression coefficient $\beta_1^{(q)}$ (Wasko et al., 2015):

$$TPSR^{(q)} = 100\ \left(\exp \beta_1^{(q)} - 1\right) \tag{2}$$

When duration (D) (from 1 to 36 hr) was considered as a covariate in the scaling estimation, the following expressions were used (Wasko et al., 2015):

$$\log P = \beta_0^{(q)} + \beta_1^{(q)} T + \beta_2^{(q)} \log D + \beta_3^{(q)} T \log D \tag{3}$$

$$TPSR_D^{(q)} = 100\ \left[\exp\left(\beta_1^{(q)} + \beta_3^{(q)} \log D\right) - 1\right] \tag{4}$$

Two 75-year periods were considered: (a) 1956–2030 (historical) and (b) 2025–2099 (future). The 1-hr AM (May to September) series were extracted from hourly rainfall series, and corresponding REs were identified. Annual maximums were then classified according to the corresponding RE duration (SDE, MDE or LDE) and the event total rainfall depth estimated.

As in PB21, a 3 × 3 grid-point pooling strategy was adopted (each grid point was examined by pooling all nine grid points within this configuration) to improve the sampling (Li, Zwiers, Zhang, & Li, 2019). No significant differences in temperature and precipitation distributions were observed at this spatial scale, as opposed to situations where pooling over large regions is considered, resulting in super CC artifact (Visser et al., 2021). The TPSRs were estimated by applying QR to the sample obtained after pooling the AM rainfall series from the 50-member ensemble. This approach differs from the one used in PB21, where the scaling was estimated for each CRCM5-LE member and averaged over the 50-member ensemble. Pooling AM series from the 50-member ensemble was preferred to the one of PB21 because the proportion of events of different durations changes across the domain (see Figure S1 in Supporting Information S1), with smaller numbers of SDE in the northern

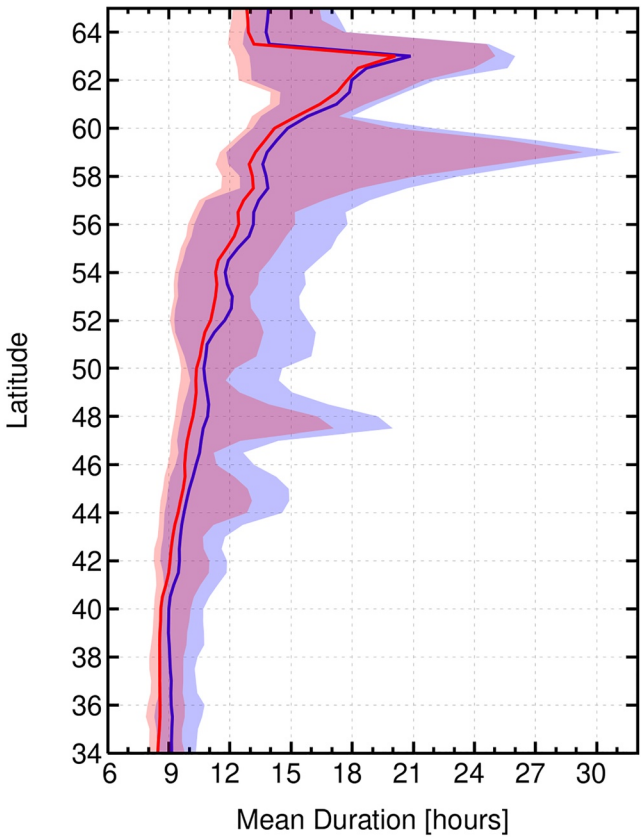

Figure 2. Longitudinal distribution of the land grid-point mean duration (hours) of RE associated with 1-hr AM for 1956–2030 (in blue) and 2025–2099 period (in red). Bold lines correspond to the median of the distribution and shaded areas to the 5%–95% percentile intervals. Latitude bins are overlapping over 0.5° and are 1° wide.

regions. Pooling increased the sample size and enabled a better estimation of QR parameters. Furthermore, estimation of the TPSR in PB21 was based on a Generalized Extreme Value distribution with temperature-dependent location and scale parameters (Zhang et al., 2017).

3. Results and Discussion

3.1. Duration of Rainfall Events Associated to 1-hr Annual Maxima

RE duration was considered as it is expected that shorter REs are more dominantly convective and that this convective character will be more pronounced as temperature increases. The consequence is that 1-hr AM embedded in a short RE will likely be more and more dominantly convective as temperature increases.

Figure 2 presents the longitudinal distributions of the mean values of RE duration associated with 1-hr AM over the two periods. As can be seen, the mean RE duration decreases moving southward. It can be related to the overall shift of 1-hr AM RE from dominantly stratiform RE in the north to dominantly convective RE in the south. Mean RE duration slightly decreases in the future period over the whole domain as well as the dispersion of the distribution, meaning that 1-hr AM will be associated with shorter and more predominantly convective RE in future climate, a result already reported by, for example, Westra et al. (2014), Panthou et al. (2014), Fowler et al. (2021), Wasko et al. (2021).

The percentages of RE belonging to the SDE, MDE, and LDE were also estimated (Figure S1 in Supporting Information S1). It clearly shows that moving southward, the percentage of 1-hr AM embedded in LDE decreases while the percentages of those embedded in SDE and MDE increase for both periods. It should be noted, however, that even in the southernmost region, significant percentages of 1-hr AM, ranging from 25% to 50%, can be embedded in LDE or MDE over both periods. The fraction of SDE (LDE) increases (decreases) for southern regions in a future climate, suggesting an intensification of dominantly-convective events. In contrast, the percentages of MDE events remain similar for both periods.

To check if more extreme 1-hr AM are embedded in shorter RE, distributions like those of Figure 2 were constructed for RE associated with 1-hr AM above given percentiles. Results show that as 1-hr AM becomes more extreme (higher percentiles), mean durations of corresponding RE decrease over both periods (Figure S2 in Supporting Information S1). Therefore more extreme 1-hr AM are embedded in shorter and more predominantly convective RE over all latitudes and for both periods.

3.2. TPSRs Without Event Duration Covariate

The TPSR was first estimated for the RE maximum intensity, which corresponds to the 1-hr AM, and then for the total rainfall depth of the corresponding RE. TPSR values were computed for both periods, over the entire domain without considering event duration as covariate (Equations 1 and 2).

Figure 3 shows the maps for the 1-hr AM TPSR and the difference with the total rainfall depth TPSR values (1-hr AM scaling minus total rainfall depth scaling) for the 50th and 99th percentiles and both periods. TPSR values for the 50th percentile of the 1-hr AM are mainly larger than the CC scaling and reach 14%/°C in the southern regions over both periods, which is consistent with the corresponding results reported by PB21. Results for the 99th percentile 1-hr AM TPSRs values are entirely different, with values globally close to the CC scaling and a much noisier spatial distribution.

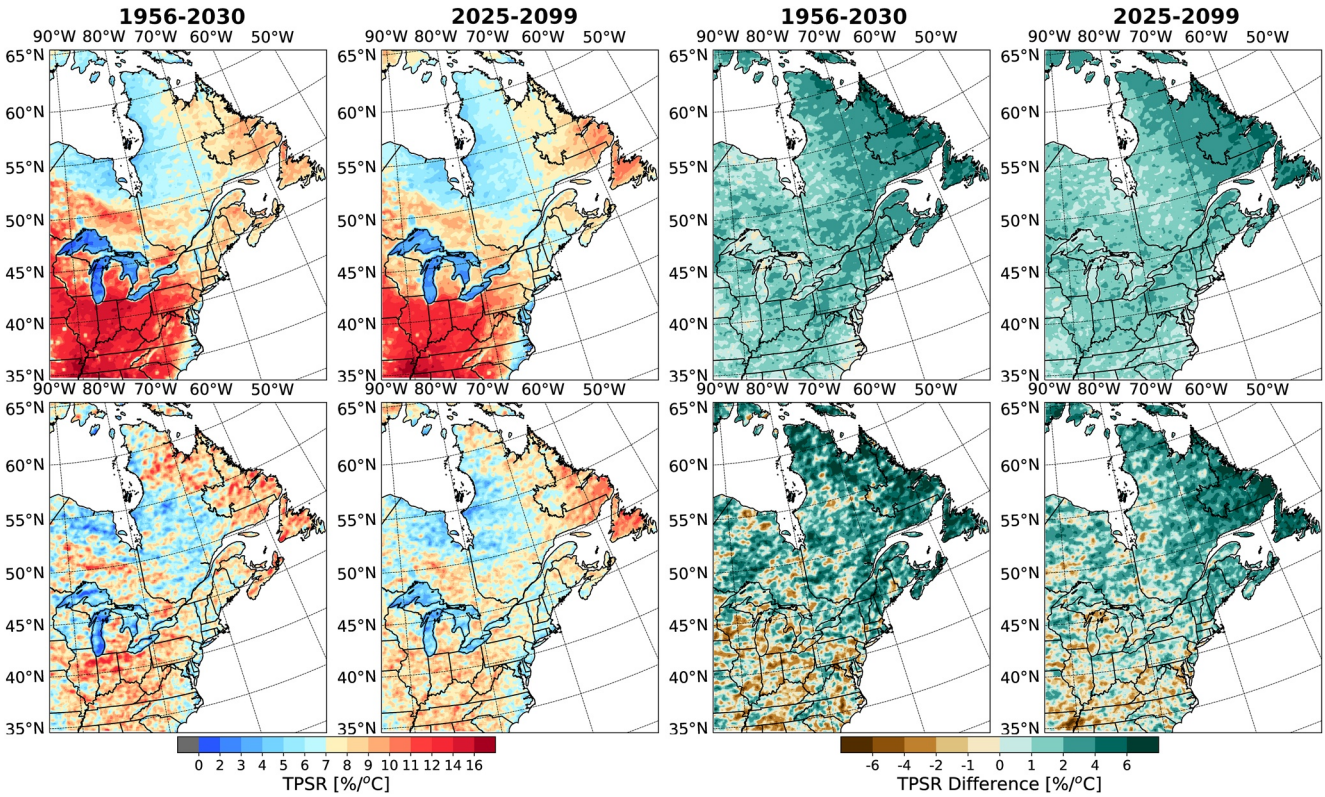

Figure 3. Maps of the 1-hr AM TPSR (columns 1 and 2) and maps of the differences between the 1-hr AM and total rainfall depth scaling (1-hr AM scaling minus total rainfall depth scaling; columns 3 and 4) over the 1956–2030 (columns 1 and 3) and 2025–2099 (columns 2 and 4) periods for the 50th percentile (first row) and the 99th percentile (second row).

Figure 3 also shows that, for the 50th percentile and both periods, 1-hr AM scaling values are larger than those of the total rainfall depth of the associated RE over most of the domain, especially in the northeastern regions. These differences range from −0.2%/° to 5.4%/°C over the domain, with an average value of 1.9%/°C. The situation is very different for the 99th percentile, where, despite a noisier global pattern, northern regions display larger TPSR values for 1-hr AM and southern regions larger TPSR for total rainfall depth of the associated RE. No apparent differences between the 1-hr AM TPSR and corresponding TPSR of the RE are observed between the future (2025–2099) and historical (1956–2030) periods.

These results provide insights on how the 1-hr AMs scale compared to the total rainfall depth of the RE in which they are embedded. For the 50th percentile 1-hr AM, peak values are more sensitive to temperature changes than the event total rainfall depth leading to an intensification of the 1-hr peak value, resulting in more peaked RE as temperature increases. The situation is different for the 99th percentile 1-hr AM where northern and southern parts of the domain display contrasting results because RE 1-hr peak values are more sensitive to temperature increases in the northern part than for the 50th percentile 1-hr AM. In contrast, in many parts of the southern region, both for historical and future periods, RE peak values are less sensitive to temperature changes than the total rainfall depth of the associated RE (see Figure S3 in Supporting Information S1). It suggests a more significant "intensification" of the whole RE than its 1-hr peak values. This shows that the scaling depends on event characteristics (e.g., RE event duration, the maximum intensity and the total rainfall depth) and the importance of including these in the temperature-precipitation scaling analysis.

3.3. TPSRs Considering Event Duration as Covariate

RE duration was then considered as a covariate when estimating TPSR (Equations 3 and 4). Figure 4 shows the median values of the longitudinal distribution of the TPSR land grid-box values for the 1-hr AM as a function of latitude and RE durations for both periods. Median TPSR values for the 50th percentiles range from 5%/°

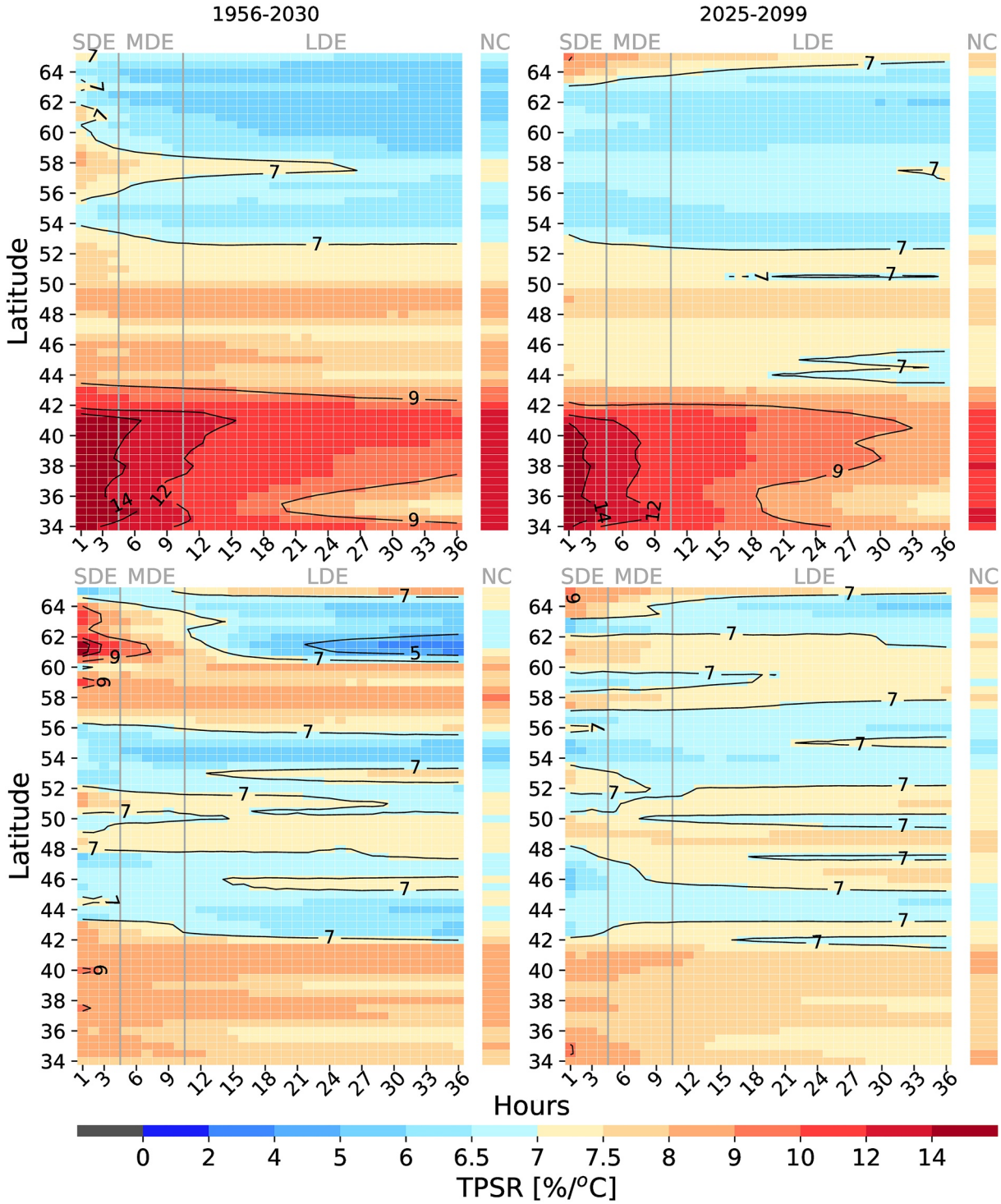

Figure 4. Median of the longitudinal distribution of TPSR land grid-box values at given latitudes for the 50th percentile (top row) and 99th percentile (bottom row) of the 1-hr AM as a function of RE duration. Vertical gray lines delineate the SDE, MDE, and LDE duration categories. The historical period (1956–2030) is displayed on the left column and the future period (2025–2099) on the right column. The corresponding median TPSR when duration is not used as a covariate (NC) is shown in the column on the right side of each graph. Latitude bins are overlapping over 0.5° and are 1° wide.

to 7%/°C) in region above 51° of latitude, and from 7%/° to 9%/°C for the central region (top row of Figure 4). Regions south of the 43° of latitude display a super CC scaling, with the largest values close to 14%/°C observed for short duration REs. Duration seems to have a relatively small impact on the TPSR values for the central and

northern regions. In contrast, a significant decrease in TPSR values for the southern region is observed as duration increases. This feature will be even more pronounced in the future. It shows that the 50th percentile 1-hr AM TPSR strongly depends on related RE duration.

Corresponding TPSR values for the 99th percentiles are displayed in Figure 4 (bottom row). Median TPSR values are close to the CC scaling for almost all durations and land grid-boxes in central and northern regions. TPSRs in southern regions are slightly above the CC scaling and lightly decrease with duration, which is very different from what has been observed for the 50th percentile. Similar results are obtained for both periods.

Super CC scaling, more specifically close to $2 \times$ CC scaling, is observed in the southern part of the domain for the 50th percentiles 1-hr AM embedded in short duration RE. Such a feature is not observed in the 99th percentile. An analysis of the corresponding results for 1-hr AM percentiles between 50th and 99th percentiles was made (see Figure S4 in Supporting Information S1). It confirms a progressive change from larger TPSR values and strong dependence on event duration for the 50th percentiles to smaller TPSR values and weak dependence on event duration as more extreme 1-hr AM are considered.

Temperature sensitivity is, therefore, larger for less extreme 1-hr AM embedded in short duration RE, reaching up to $2 \times$ CC scaling in some regions (see Figure 3). How to interpret these results? First, if the 1-hr AM is more extreme (higher percentiles), it is likely associated with a more convective dominant RE no matter the duration of the associated RE. In that case, it can be expected that the temperature dependence will closely match the CC scaling as observed for the 99th percentile 1-hr AM in the southern part of the domain. However, less extreme 1-hr AM (e.g., 50th percentile) can be embedded in less dominant convective RE. In that case, the convective character of the 1-hr AM and the associated RE will likely increase with temperature for short-duration REs resulting in super CC scaling (shorter RE becomes more convective-dominant as temperature increases). It is observed in the southern part of the domain, as the percentages of 1-hr AM associated with SDE increases to a value close to 20% when super CC is observed (see Figure S1 in Supporting Information S1). Transitions to super CC scaling were reported for a fraction of convective precipitation around 20% by Berg et al. (2013), Park & Min (2017). Although a fraction of 20% of 1-hr AM embedded in SDE does not mean a 20% fraction of convective precipitation, it is interesting to note that in both cases, some threshold value related to the convective character of the RE (here, the duration) is needed to trigger a transition to super CC.

Figure 4 also shows the longitudinal median TPSR values when event duration is not considered (right-hand side columns of each panel). In the southern region where TPSR changes with RE duration, TPSR values are close to the observed scaling for the MDE and significantly larger than the CC-scaling since most of the 1-hr AMs are associated with MDE (see Figure S1 in Supporting Information S1). These results show that the TPSR of the 1-hr AM for the most extreme events, like those corresponding to the 99th percentile, are less affected by the duration of the events in which they are embedded. The TPSR values are, therefore, closer to the CC-scaling.

Similar patterns are observed for the TPSR of corresponding total rainfall depth (Figure S5 in Supporting Information S1). Super CC scaling is observed in the southern region for the 50th percentile with a strong dependence on duration. A transition to super CC scaling is also observed at around 43° of latitude moving southward for both the 50th and 99th percentiles. Furthermore, the scaling when no covariate is included reflects the most likely precipitation events group (MDE in this case; see Figure S1 in Supporting Information S1).

Figure 5 shows the differences between TPSRs for 1-hr AM and for corresponding total rainfall depth values (1-hr AM scaling minus total rainfall depth scaling). Differences are mostly positive (1-hr AM scaling is higher than the total rainfall depth scaling) for the 50th percentile over all the domain and lightly increase as duration increases with values slightly above 2%/°C for the longest storm duration. For the 99th percentile 1-hr AM, Figure 5 (bottom panel) reveals very contrasting patterns for the north and south regions. Northern regions are characterized by higher 1-hr AM TPSR values, while southern regions (below 45° of latitude) display larger total rainfall depth TPSR values with for both regions slight increases as duration increases.

This last result suggests that in southern regions, where the convective character of the whole RE is more pronounced, increasing temperature reinforces the convective character of the whole RE. It follows that the TPSR of the RE is larger than the corresponding value for 1-hr AM, and super CC scaling is observed for the total rainfall depth (see Figure S5 in Supporting Information S1). It is not the case for the northern regions where 1-hr AM are more likely embedded in less-dominantly convective MDE and LDE (see Figure S1 in Supporting Information S1). Therefore the 1-hr RE peak encompasses the dominant convective part of the RE and is more sensitive

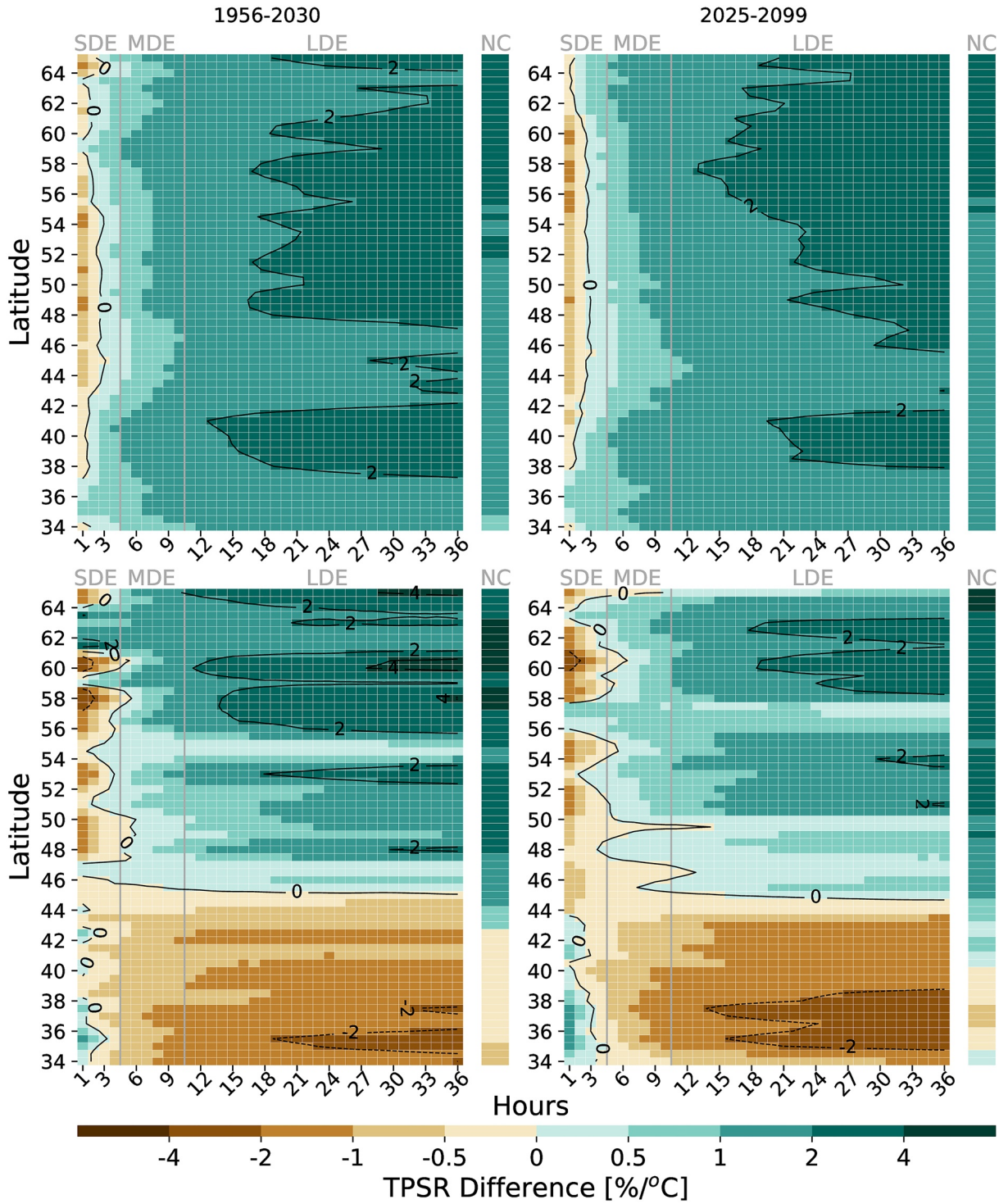

Figure 5. Median of the distribution of TPSR difference (1-hr AM scaling minus total rainfall depth scaling) for the 50th percentile (top panel) and 99th percentile (bottom panel) (for each latitude bin) as a function of event duration. Vertical gray lines delineate the three categories used; SDE, MDE, and LDE. Historical (future) period in the left (right). On the right side of each period is included the corresponding median TPSR without including the storm duration as a covariate (NC). Latitude bins are overlapping over 0.5° and are 1° wide.

to temperature changes than the whole RE, except for the more-dominantly convective SDE where RE TPSRs are larger than the corresponding 1-hr AM.

4. Conclusions

Temperature-precipitation scaling rates were estimated for both 1-hr AM (May to September), and total rainfall depth of corresponding REs in which these AM are embedded. A MIT of 3 hr and a 0.1 mm threshold for wet hours were considered. RE duration was used as a proxy to assess the convective character of the RE, assuming that a shorter RE is more likely convective. Simulations from the 50-member Canadian Regional Climate Model Large Ensemble (CRCM5-LE) over Northeastern North America for the 1950–2099 period were used. Two sub-periods, 1956–2030 and 2025–2099 were defined. TPSRs were estimated using QR.

Results showed that the mean latitudinal RE duration associated with 1-hr AM decreases moving southward. It suggests that 1-hr AMs are associated with dominantly stratiform REs in the north and more dominantly convective REs in the south. Also, mean RE duration globally decreases in the future period over the whole domain, suggesting that 1-hr AM will be embedded in shorter REs in a future climate. This study confirms previously reported results that more extreme 1-hr AM should be expected in a future climate and that they will be associated with presumably more dominantly convective RE (see e.g., Fowler et al., 2021; Wasko et al., 2021; Westra et al., 2014).

TPSR estimates for the 50th and 99th percentiles of the 1-hr AM distributions and corresponding RE were estimated and compared. Differences in the scaling (1-hr AM scaling minus total rainfall depth scaling) showed positive values for the entire domain for moderate events and increased when storm duration increased. It suggests the intensification of events generating more rainfall with a more dominant contribution from its 1-h peak value for those events. Comparison of TPSR values for 1-hr AM and total rainfall depth of associated RE also revealed distinctive features between northern and southern regions for the 99th percentile. Thus 1-hr AM TPSR values are larger than the TPSR values for the total rainfall depth north of the 45° of latitude, while the opposite situation is observed south of this latitude. Therefore for the southern regions, since the convective character of the RE is more pronounced, increasing temperature increases the convective character of the whole RE resulting in larger TPSR values for the total rainfall depth of the RE. In northern regions, where 1-hr AM is embedded in less-dominantly convective RE, 1-hr AM is more sensitive to temperature changes than the whole RE resulting in larger 1-hr AM TPSR than the total rainfall depth of the associated RE.

Storm duration plays a crucial role in the estimated TPSR since it determines the more or less convective character of the RE in which 1-hr AMs are embedded. TPSRs estimated without using storm duration as a covariate will be representative of the dominant precipitation event duration (MDE in this case).

Super CC scaling (>7%/°C), reaching values close to 2 × CC (for SDE) scaling in the southern part of the domain, was observed for both periods for the 50th percentile 1-hr AM. Strong dependence of estimated TPSR with RE duration was also observed for the 50th percentile 1-hr AM over southern regions. This dependence on RE duration progressively disappeared as more extreme 1-hr AMs were considered. Incidentally, TPSR for the 99th percentile 1-hr AM depends weakly on RE duration with values slightly above the CC scaling. The already extreme and convective nature of the 99th percentile 1-hr AM and associated RE, even at lower temperatures, may explain this result. The strong dependence of 50th percentile 1-hr AM to RE duration was related to the increasing convective character of the RE and the embedded 1-hr AM as temperature increases. It can be assimilated to a shift from a more large-scale type RE to a more convective RE as temperature increases.

The transition to super CC moving southward occurs when the percentage of 1-hr AM associated with SDE (<5 hr) increases to reach a value close to 20%. It is interesting to note that other studies also reported a transition to super CC when the fraction of convective precipitation reaches some threshold. For instance (Park & Min, 2017), reports a transition from CC to super CC scaling when the fraction of convective events reaches a value close to 0.2 (a similar result was obtained in Germany by Berg et al. (2013).

The Large Ensemble (CRCM5-LE) considered in this study, as was mentioned in Section 2, is a parameterized convection model (PCM). The fact that this RCM does not explicitly resolve convective processes must be kept in mind when interpreting these results. Such representation was indeed related to some inaccuracies in the simulated diurnal cycle of precipitation during summer months (Ban et al., 2015), as well as underestimation of dry

days and bias in the simulated frequency of light REs (Kendon et al., 2012). Convection-permitting models (CPM, spatial resolution ≤4 km) in which deep convection is explicitly resolved have been developed over recent years (Kendon et al., 2012; Prein et al., 2015). These models overcome many of the limitations of PCMs mentioned above (Ban et al., 2015). However, CPM's high temporal and spatial resolutions translate into high computational costs. In this context, regional PCMs can provide many simulations (large ensembles) over extended periods (Fosser et al., 2017) enabling robust estimates of TPSRs (Li, Zwiers, Zhang, & Li, 2019).

Fowler et al. (2021) listed the different processes associated to deep convection that could enhance the intensification of sub-daily rainfall extremes and lead to super CC scaling. They conclude that CPMs project higher intensification of sub-daily extreme rainfall than PCM. Although these processes are not explicitly resolved in a PCM, our results suggest that, even when CPM is used to assess the TPSR of extreme rainfall, it is essential to consider the associated RE. Such an event-based approach provides a more comprehensive framework to disentangle the contribution to super CC resulting from a shift from stratiform to convective rainfall (see Figure 3 of Fowler et al., 2021) to the one resulting from an intensification of the convection itself.

Comparing the TPSR values from 1-hr peak RE and total rainfall depth of the related RE may also have major hydrological impacts, especially in urban areas and for flash floods. Results support the conclusion that for the southern part of the domain where convective REs are dominant, the TPSR of total rainfall depth RE associated with the most extreme 1-hr AM will be higher than the corresponding 1-hr peak value. Therefore the "intensification" of the whole RE will be larger than its 1-hr peak value with TPSR values close to 10%/°C no matter the duration of the related RE. It may lead to considerable increases in total event rainfall associated to 1-hr AM and increasing flood risks. This result may also have important consequences as AM intensities, through Intensity-Duration-Frequency (IDF) curves, are usually used to design many hydraulic infrastructures (Mailhot & Duchesne, 2010). Various approaches and values have been proposed to update IDF curves to consider the possible impacts of climate change on extreme rainfall (see Martel et al. (2021) for an overview). Accounting of CC by upgrading IDF values assumed implicitly that REs would intensify similarly to the AMs in which they are embedded. Actual results show that this will not be the case for most extreme rainfall; therefore, such increases in AM could underestimate the RE's corresponding impact.

Data Availability Statement

The CRCM5-LE data set from the Climex project (ClimEx, 2019; Leduc et al., 2019) was used in the creation of this manuscript.

Acknowledgments
The authors would like to express their gratitude to the anonymous reviewers whose suggestions contributed to elevate the quality of the manuscript. Alain Mailhot thanks the Discovery Grants Program from the Natural Science and Engineering Research Council of Canada (NSERC) for providing financial support for this project. The authors thank the consortium Ouranos who gave access to the CRCM5-LE. The production of ClimEx was funded within the ClimEx project by the Bavarian State Ministry for the Environment and Consumer Protection. The CRCM5 was developed by the ESCER centre of Université du Québec à Montréal (UQAM; www.escer.uqam.ca) in collaboration with Environment and Climate Change Canada. We acknowledge Environment and Climate Change Canada's Canadian Centre for Climate Modelling and Analysis for executing and making available the CanESM2 Large Ensemble simulations used in this study and the Canadian Sea Ice and Snow Evolution Network for proposing the simulations. Computations with the CRCM5 for the ClimEx project were made on the SuperMUC supercomputer at Leibniz Supercomputing Centre (LRZ) of the Bavarian Academy of Sciences and Humanities. The operation of this supercomputer is funded via the Gauss Centre for Supercomputing (GCS) by the German Federal Ministry of Education and Research and the Bavarian State Ministry of Education, Science and the Arts.

References

Alduchov, O. A., & Eskridge, R. E. (1996). Improved magnus form approximation of saturation vapor pressure. *Journal of Applied Meteorology*, *35*(4), 601–609. https://doi.org/10.1175/1520-0450(1996)035<0601:imfaos>2.0.co;2

Ali, H., Fowler, H. J., & Mishra, V. (2018). Global observational evidence of strong linkage between dew point temperature and precipitation extremes. *Geophysical Research Letters*, *45*(22), 12320–12330. https://doi.org/10.1029/2018GL080557

Arora, V. K., Scinocca, J. F., Boer, G. J., Christian, J. R., Denman, K. L., Flato, G. M., et al. (2011). Carbon emission limits required to satisfy future representative concentration pathways of greenhouse gases. *Geophysical Research Letters*, *38*(5), L05805. https://doi.org/10.1029/2010GL046270

Ban, N., Schmidli, J., & Schär, C. (2015). Heavy precipitation in a changing climate: Does short-term summer precipitation increase faster? *Geophysical Research Letters*, *42*(4), 1165–1172. https://doi.org/10.1002/2014GL062588

Bélair, S., Mailhot, J., Girard, C., & Vaillancourt, P. (2005). Boundary layer and shallow cumulus clouds in a medium-range forecast of a large-scale weather system. *Monthly Weather Review*, *133*(7), 1938–1960. https://doi.org/10.1175/MWR2958.1

Berg, P., & Haerter, J. O. (2013). Unexpected increase in precipitation intensity with temperature—A result of mixing of precipitation types? *Atmospheric Research*, *119*, 56–61. https://doi.org/10.1016/j.atmosres.2011.05.012

Berg, P., Haerter, J. O., Thejll, P., Piani, C., Hagemann, S., & Christensen, J. H. (2009). Seasonal characteristics of the relationship between daily precipitation intensity and surface temperature. *Journal of Geophysical Research*, *114*(D18), D18102. https://doi.org/10.1029/2009JD012008

Berg, P., Moseley, C., & Haerter, J. O. (2013). Strong increase in convective precipitation in response to higher temperatures. *Nature Geoscience*, *6*(3), 181–185. https://doi.org/10.1038/ngeo1731

Chernokulsky, A., Kozlov, F., Zolina, O., Bulygina, O., Mokhov, I. I., & Semenov, V. A. (2019). Observed changes in convective and stratiform precipitation in Northern Eurasia over the last five decades. *Environmental Research Letters*, *14*(4), 045001. https://doi.org/10.1088/1748-9326/aafb82

ClimEx. (2019). ClimEx project: A 50-member ensemble of climate change projections; fifth version of the canadian regional climate model—Large ensemble (CRCM5-LE). [Dataset]. Climex Project. Retrieved from https://www.climex-project.org/en/data-access/

Drobinski, P., Alonzo, B., Bastin, S., Silva, N. D., & Muller, C. (2016). Scaling of precipitation extremes with temperature in the French Mediterranean region: What explains the hook shape? *Journal of Geophysical Research: Atmospheres*, *121*(7), 3100–3119. https://doi.org/10.1002/2015JD023497

Dunkerley, D. (2008). Identifying individual rain events from pluviograph records: A review with analysis of data from an Australian dryland site. *Hydrological Processes*, *22*(26), 5024–5036. https://doi.org/10.1002/hyp.7122

Dunkerley, D. (2015). Intra-event intermittency of rainfall: An analysis of the metrics of rain and no-rain periods. *Hydrological Processes*, *29*(15), 3294–3305. https://doi.org/10.1002/hyp.10454

Fischer, A. M., Keller, D. E., Liniger, M. A., Rajczak, J., Schär, C., & Appenzeller, C. (2015). Projected changes in precipitation intensity and frequency in Switzerland: A multi-model perspective. *International Journal of Climatology*, *35*(11), 3204–3219. https://doi.org/10.1002/joc.4162

Fosser, G., Khodayar, S., & Berg, P. (2017). Climate change in the next 30 years: What can a convection-permitting model tell us that we did not already know? *Climate Dynamics*, *48*(5), 1987–2003. https://doi.org/10.1007/s00382-016-3186-4

Fowler, H. J., Lenderink, G., Prein, A. F., Westra, S., Allan, R. P., Ban, N., et al. (2021). Anthropogenic intensification of short-duration rainfall extremes. *Nature Reviews Earth & Environment*, *2*(2), 107–122. https://doi.org/10.1038/s43017-020-00128-6

Fyfe, J. C., Derksen, C., Mudryk, L., Flato, G. M., Santer, B. D., Swart, N. C., et al. (2017). Large near-term projected snowpack loss over the western United States. *Nature Communications*, *8*(1), 14996. https://doi.org/10.1038/ncomms14996

Gaál, L., Molnar, P., & Szolgay, J. (2014). Selection of intense rainfall events based on intensity thresholds and lightning data in Switzerland. *Hydrology and Earth System Sciences*, *18*(5), 1561–1573. https://doi.org/10.5194/hess-18-1561-2014

Gao, X., Zhu, Q., Yang, Z., Liu, J., Wang, H., Shao, W., & Huang, G. (2018). Temperature dependence of hourly, daily, and event-based precipitation extremes over China. *Scientific Reports*, *8*(1), 17564. https://doi.org/10.1038/s41598-018-35405-4

Haerter, J. O., & Berg, P. (2009). Unexpected rise in extreme precipitation caused by a shift in rain type? *Nature Geoscience*, *2*(6), 372–373. https://doi.org/10.1038/ngeo523

Hand, W. H., Fox, N. I., & Collier, C. G. (2004). A study of twentieth-century extreme rainfall events in the United Kingdom with implications for forecasting. *Meteorological Applications*, *11*(1), 15–31. https://doi.org/10.1017/S1350482703001117

Hardwick Jones, R., Westra, S., & Sharma, A. (2010). Observed relationships between extreme sub-daily precipitation, surface temperature, and relative humidity. *Geophysical Research Letters*, *37*(22), L22805. https://doi.org/10.1029/2010GL045081

Hatsuzuka, D., Sato, T., & Higuchi, Y. (2021). Sharp rises in large-scale, long-duration precipitation extremes with higher temperatures over Japan. *Npj Climate and Atmospheric Science*, *4*(1), 29. https://doi.org/10.1038/s41612-021-00184-9

Ivancic, T. J., & Shaw, S. B. (2016). A U.S.-based analysis of the ability of the Clausius-Clapeyron relationship to explain changes in extreme rainfall with changing temperature. *Journal of Geophysical Research: Atmospheres*, *121*(7), 3066–3078. https://doi.org/10.1002/2015JD024288

Kain, J. S., & Fritsch, J. M. (1990). A one-dimensional entraining/detraining plume model and its application in convective parameterization. *Journal of the Atmospheric Sciences*, *47*(23), 2784–2802. https://doi.org/10.1175/1520-0469(1990)047<2784:aodepm>2.0.co;2

Kendon, E. J., Roberts, N. M., Senior, C. A., & Roberts, M. J. (2012). Realism of rainfall in a very high-resolution regional climate model. *Journal of Climate*, *25*(17), 5791–5806. https://doi.org/10.1175/JCLI-D-11-00562.1

Koenker, R. (2005). *Quantile regression*. Cambridge University Press. https://doi.org/10.1017/CBO9780511754098

Koenker, R., & Bassett, G. (1978). Regression quantiles. *Econometrica*, *46*(1), 33–50. https://doi.org/10.2307/1913643

Koenker, R., Portnoy, S., Ng, P. T., Melly, B., Zeileis, A., Grosjean, P., et al. (2022). Quantreg: Quantile regression, R package version 5.88. Retrieved from https://CRAN.R-project.org/package=quantreg

Kunkel, K. E., Easterling, D. R., Kristovich, D. A. R., Gleason, B., Stoecker, L., & Smith, R. (2012). Meteorological causes of the secular variations in observed extreme precipitation events for the conterminous United States. *Journal of Hydrometeorology*, *13*(3), 1131–1141. https://doi.org/10.1175/JHM-D-11-0108.1

Kuo, H. L. (1965). On formation and intensification of tropical cyclones through latent heat release by cumulus convection. *Journal of the Atmospheric Sciences*, *22*(1), 40–63. https://doi.org/10.1175/1520-0469(1965)022<0040:ofaiot>2.0.co;2

Kyselý, J., Rulfová, Z., Farda, A., & Hanel, M. (2016). Convective and stratiform precipitation characteristics in an ensemble of regional climate model simulations. *Climate Dynamics*, *46*(1), 227–243. https://doi.org/10.1007/s00382-015-2580-7

Lawrence, M. G. (2005). The relationship between relative humidity and the dewpoint temperature in moist air: A simple conversion and applications. *Bulletin of the American Meteorological Society*, *86*(2), 225–234. https://doi.org/10.1175/BAMS-86-2-225

Leduc, M., Mailhot, A., Frigon, A., Martel, J.-L., Ludwig, R., Brietzke, G. B., et al. (2019). The ClimEx project: A 50-member ensemble of climate change projections at 12-km resolution over Europe and northeastern North America with the Canadian regional climate model (CRCM5). *Journal of Applied Meteorology and Climatology*, *58*(4), 663–693. https://doi.org/10.1175/JAMC-D-18-0021.1

Lenderink, G., & Meijgaard, E. (2008). Increase in hourly precipitation extremes beyond expectations from temperature changes. *Nature Geoscience*, *1*(8), 511–514. https://doi.org/10.1038/ngeo262

Lenderink, G., & Meijgaard, E. v. (2009). Unexpected rise in extreme precipitation caused by a shift in rain type? *Nature Geoscience*, *2*(6), 373. https://doi.org/10.1038/ngeo524

Lenderink, G., & Meijgaard, E. v. (2010). Linking increases in hourly precipitation extremes to atmospheric temperature and moisture changes. *Environmental Research Letters*, *5*(2), 025208. https://doi.org/10.1088/1748-9326/5/2/025208

Lenderink, G., Mok, H. Y., Lee, T. C., & Oldenborgh, G. J. v. (2011). Scaling and trends of hourly precipitation extremes in two different climate zones—Hong Kong and The Netherlands. *Hydrology and Earth System Sciences*, *15*(9), 3033–3041. https://doi.org/10.5194/hess-15-3033-2011

Li, C., Zwiers, F., Zhang, X., Chen, G., Lu, J., Li, G., et al. (2019). Larger increases in more extreme local precipitation events as climate warms. *Geophysical Research Letters*, *46*(12), 6885–6891. https://doi.org/10.1029/2019GL082908

Li, C., Zwiers, F., Zhang, X., & Li, G. (2019). How much information is required to well constrain local estimates of future precipitation extremes? *Earth's Future*, *7*(1), 11–24. https://doi.org/10.1029/2018EF001001

Llasat, M. C., Rigo, T., Ceperuelo, M., & Barrera, A. (2005). Estimation of convective precipitation: The meteorological radar versus an automatic rain gauge network. *Advances in Geosciences*, *2*, 103–109. https://doi.org/10.5194/adgeo-2-103-2005

Loriaux, J. M., Lenderink, G., Roode, S. R. D., & Siebesma, A. P. (2013). Understanding convective extreme precipitation scaling using observations and an entraining plume model. *Journal of the Atmospheric Sciences*, *70*(11), 3641–3655. https://doi.org/10.1175/JAS-D-12-0317.1

Maeda, E. E., Utsumi, N., & Oki, T. (2012). Decreasing precipitation extremes at higher temperatures in tropical regions. *Natural Hazards*, *64*(1), 935–941. https://doi.org/10.1007/s11069-012-0222-5

Mailhot, A., & Duchesne, S. (2010). Design Criteria of urban Drainage infrastructures under climate change. *Journal of Water Resources Planning and Management*, *136*, 201–208. https://doi.org/10.1061/(ASCE)WR.1943-5452.0000023

Martel, J.-L., Brissette, F. P., Lucas-Picher, P., Troin, M., & Arsenault, R. (2021). Climate change and rainfall intensity–duration–frequency curves: Overview of science and guidelines for adaptation. *Journal of Hydrologic Engineering*, *26*(10), 03121001. https://doi.org/10.1061/(ASCE)HE.1943-5584.0002122

Martinkova, M., & Hanel, M. (2016). Evaluation of relations between extreme precipitation and temperature in observational time series from the Czech Republic. *Advances in Meteorology*, *2016*, e2975380. https://doi.org/10.1155/2016/2975380

Martynov, A., Laprise, R., Sushama, L., Winger, K., Šeparović, L., & Dugas, B. (2013). Reanalysis-driven climate simulation over CORDEX North America domain using the Canadian Regional Climate Model, version 5: Model performance evaluation. *Climate Dynamics*, *41*(11), 2973–3005. https://doi.org/10.1007/s00382-013-1778-9

Mishra, V., Wallace, J. M., & Lettenmaier, D. P. (2012). Relationship between hourly extreme precipitation and local air temperature in the United States. *Geophysical Research Letters*, *39*(16), L16403. https://doi.org/10.1029/2012GL052790

Molnar, P., Fatichi, S., Gaál, L., Szolgay, J., & Burlando, P. (2015). Storm type effects on super Clausius–Clapeyron scaling of intense rainstorm properties with air temperature. *Hydrology and Earth System Sciences*, *19*(4), 1753–1766. https://doi.org/10.5194/hess-19-1753-2015

Panthou, G., Mailhot, A., Laurence, E., & Talbot, G. (2014). Relationship between surface temperature and extreme rainfalls: A multi-time-scale and event-based analysis. *Journal of Hydrometeorology*, *15*(5), 1999–2011. https://doi.org/10.1175/JHM-D-14-0020.1

Park, I.-H., & Min, S.-K. (2017). Role of convective precipitation in the relationship between subdaily extreme precipitation and temperature. *Journal of Climate*, *30*(23), 9527–9537. https://doi.org/10.1175/JCLI-D-17-0075.1

Penide, G., Protat, A., Kumar, V. V., & May, P. T. (2013). Comparison of two convective/stratiform precipitation classification techniques: Radar reflectivity texture versus drop size distribution–based approach. *Journal of Atmospheric and Oceanic Technology*, *30*(12), 2788–2797. https://doi.org/10.1175/JTECH-D-13-00019.1

Pérez Bello, A., Mailhot, A., & Paquin, D. (2021). The response of daily and sub-daily extreme precipitations to changes in surface and dew-point temperatures. *Journal of Geophysical Research: Atmospheres*, *126*(16), e2021JD034972. https://doi.org/10.1029/2021JD034972

Prein, A. F., Langhans, W., Fosser, G., Ferrone, A., Ban, N., Goergen, K., et al. (2015). A review on regional convection-permitting climate modeling: Demonstrations, prospects, and challenges. *Reviews of Geophysics*, *53*(2), 323–361. https://doi.org/10.1002/2014RG000475

Riahi, K., Rao, S., Krey, V., Cho, C., Chirkov, V., Fischer, G., et al. (2011). RCP 8.5—A scenario of comparatively high greenhouse gas emissions. *Climatic Change*, *109*(1), 33–57. https://doi.org/10.1007/s10584-011-0149-y

Rigo, T., & Llasat, M. C. (2004). A methodology for the classification of convective structures using meteorological radar: Application to heavy rainfall events on the Mediterranean coast of the Iberian Peninsula. *Natural Hazards and Earth System Sciences*, *4*(1), 59–68. https://doi.org/10.5194/nhess-4-59-2004

Ruiz-Leo, A. M., Hernández, E., Queralt, S., & Maqueda, G. (2013). Convective and stratiform precipitation trends in the Spanish Mediterranean coast. *Atmospheric Research*, *119*, 46–55. https://doi.org/10.1016/j.atmosres.2011.07.019

Rulfová, Z., & Kyselý, J. (2013). Disaggregating convective and stratiform precipitation from station weather data. *Atmospheric Research*, *134*, 100–115. https://doi.org/10.1016/j.atmosres.2013.07.015

Šeparović, L., Alexandru, A., Laprise, R., Martynov, A., Sushama, L., Winger, K., et al. (2013). Present climate and climate change over North America as simulated by the fifth-generation Canadian regional climate model. *Climate Dynamics*, *41*(11), 3167–3201. https://doi.org/10.1007/s00382-013-1737-5

Sigmond, M., Fyfe, J. C., & Swart, N. C. (2018). Ice-free Arctic projections under the Paris agreement. *Nature Climate Change*, *8*(5), 404–408. https://doi.org/10.1038/s41558-018-0124-y

Sundqvist, H. (1978). A parameterization scheme for non-convective condensation including prediction of cloud water content. *Quarterly Journal of the Royal Meteorological Society*, *104*(441), 677–690. https://doi.org/10.1002/qj.49710444110

Sundqvist, H., Berge, E., & Kristjánsson, J. E. (1989). Condensation and cloud parameterization studies with a mesoscale numerical weather prediction model. *Monthly Weather Review*, *117*(8), 1641–1657. https://doi.org/10.1175/1520-0493(1989)117<1641:cacpsw>2.0.co;2

Svoboda, V., Hanel, M., Máca, P., & Kyselý, J. (2017). Characteristics of rainfall events in regional climate model simulations for the Czech Republic. *Hydrology and Earth System Sciences*, *21*(2), 963–980. https://doi.org/10.5194/hess-21-963-2017

Tremblay, A. (2005). The stratiform and convective components of surface precipitation. *Journal of the Atmospheric Sciences*, *62*(5), 1513–1528. https://doi.org/10.1175/JAS3411.1

Trenberth, K. E., Dai, A., Rasmussen, R. M., & Parsons, D. B. (2003). The changing character of precipitation. *Bulletin of the American Meteorological Society*, *84*(9), 1205–1218. https://doi.org/10.1175/BAMS-84-9-1205

Utsumi, N., Seto, S., Kanae, S., Maeda, E. E., & Oki, T. (2011). Does higher surface temperature intensify extreme precipitation? *Geophysical Research Letters*, *38*(16), L16708. https://doi.org/10.1029/2011GL048426

van Vuuren, D. P., Edmonds, J., Kainuma, M., Riahi, K., Thomson, A., Hibbard, K., et al. (2011). The representative concentration pathways: An overview. *Climatic Change*, *109*(1), 5–31. https://doi.org/10.1007/s10584-011-0148-z

Visser, J. B., Wasko, C., Sharma, A., & Nathan, R. (2020). Resolving inconsistencies in extreme precipitation-temperature sensitivities. *Geophysical Research Letters*, *47*(18), e2020GL089723. https://doi.org/10.1029/2020GL089723

Visser, J. B., Wasko, C., Sharma, A., & Nathan, R. (2021). Eliminating the "Hook" in precipitation–temperature scaling. *Journal of Climate*, *34*(23), 9535–9549. https://doi.org/10.1175/JCLI-D-21-0292.1

Wasko, C., Lu, W. T., & Mehrotra, R. (2018). Relationship of extreme precipitation, dry-bulb temperature, and dew point temperature across Australia. *Environmental Research Letters*, *13*(7), 074031. https://doi.org/10.1088/1748-9326/aad135

Wasko, C., Nathan, R., Stein, L., & O'Shea, D. (2021). Evidence of shorter more extreme rainfalls and increased flood variability under climate change. *Journal of Hydrology*, *603*, 126994. https://doi.org/10.1016/j.jhydrol.2021.126994

Wasko, C., & Sharma, A. (2014). Quantile regression for investigating scaling of extreme precipitation with temperature. *Water Resources Research*, *50*(4), 3608–3614. https://doi.org/10.1002/2013WR015194

Wasko, C., Sharma, A., & Johnson, F. (2015). Does storm duration modulate the extreme precipitation-temperature scaling relationship? *Geophysical Research Letters*, *42*(20), 8783–8790. https://doi.org/10.1002/2015GL066274

Westra, S., Fowler, H. J., Evans, J. P., Alexander, L. V., Berg, P., Johnson, F., et al. (2014). Future changes to the intensity and frequency of short-duration extreme rainfall. *Reviews of Geophysics*, *52*(3), 522–555. https://doi.org/10.1002/2014RG000464

Ye, H., Fetzer, E. J., Wong, S., & Lambrigtsen, B. H. (2017). Rapid decadal convective precipitation increase over Eurasia during the last three decades of the 20th century. *Science Advances*, *3*(1), e1600944. https://doi.org/10.1126/sciadv.1600944

Zhang, X., Zwiers, F. W., Li, G., Wan, H., & Cannon, A. J. (2017). Complexity in estimating past and future extreme short-duration rainfall. *Nature Geoscience*, *10*(4), 255–259. https://doi.org/10.1038/ngeo2911